Joint Observation of State and Topology in DC Networks

Tuncay Altun, *Student Member, IEEE,* Ramtin Madani, *Member, IEEE,* and Ali Davoudi, *Senior Member, IEEE*

***Abstract*—This paper copes with the joint state estimation and topology identification problem in direct current (DC) networks. This problem is challenging due to binary decisions and nonlinear relations between sensor measurements and state variables. We introduce a non-convex nuclear norm estimator whose non-convexity is addressed by incorporating two inertia terms. In the presence of noise, penalty terms are integrated into the objective function to estimate unknown noise values. Numerical results for the modified IEEE 9-bus, 14-bus, and 30-bus systems corroborate the merits of the proposed technique. Furthermore, this technique is experimentally validated for a converter-augmented 14-bus system in a real-time hardware-in-the-loop environment.**

***Index Terms*—Convex optimization, DC network, state estimation, topology identification.**

I. Introduction

DIRECT current (DC) networks are gaining prominence with the increasing penetration of DC-native sources, loads, and storages, since they offer improved efficiency in conversion/distribution over alternating current (AC) networks. For static distribution topologies, estimation techniques can extract the system state to be used in network analysis, control, optimization, or diagnostic under normal, emergency, or restorative operations [1]. The most recent topology information is needed to meaningfully carry out the state estimation process; any error or misconfiguration in the assumed topology could result in inappropriate control decisions [2], [3]. Incorporating statuses of the lines, that collectively describe the overall network topology, into the state estimation process is challenging as they introduce binary variables [4], [5]. Moreover, converter-populated DC networks might employ fewer sensors due to cost, security, or privacy concerns, leading to low-observability conditions.

Classical state estimation is usually solved by Gauss-Newton approaches that might converge to a local minima [6]. Convex relaxation methods can either directly solve the estimation problem [7] or provide an initial guess for the Newton's method [8]. Convergence guarantees for the estimation process using convex relaxation techniques are given in [9]. With measurement redundancy, incorporating penalty terms in the formulation of the objective function can help cleansing noise and bad data [10]–[12]. These techniques, however, assume a fixed network topology.

Topology identification is either a prerequisite to the estimation process, or should be considered concurrently. The combined problem can be solved using a Gauss-Newton method, e.g., generalized state estimation (GSE) [4], or convex relaxation methods [5]. Inverse power flow formulation can describe the network topology through a nodal admittance matrix [13]. These studies usually assume imperfect but highly-redundant measurement. Low-observability condition refers to the sparse sensor that results in an under-determined system. Additional sensors placement [14] or pseudo-measurements from existing sensors data [15] are needed, but this comes with additional cost, computational burden, or estimation errors [16]. The matrix completion method, that offers a solution to an under-determined system, has been applied to distribution networks with poor sensors installation [17], [18]. While the joint state estimation and topology identification problem has been studied for AC networks [5], its solution has not yet been elaborated under low-observability conditions [16], [19]–[22]. Moreover, state estimation and topology identification of DC networks are rare in the literature [23]–[25], and have not even considered the observability conditions.

We leverage the physical properties of DC networks to develop a polynomial-time joint estimation and topology identification algorithm using a limited number of measurement. We formulate this as a non-convex mixed-binary problem, develop a non-convex nuclear norm estimator, and address this non-convexity by using two inertia terms. The presence of zero injection buses (i.e., a bus with no load or converter) is used to strengthen the convex relaxation and decrease the number of required sensors. The resulting formulation does not rely on prior knowledge of unmonitored line-statuses, current, or power flow measurements that could infer topology information. The devised convex optimization framework is robustified against noise by upgrading to a penalized convex program. The proposed formulation is in a generic form, and can be solved with various numerical solvers.

The remainder of this paper is organized as follows. Section II gives the preliminaries. Section III defines the joint state estimation and topology identification problem for noiseless measurements. This non-convex problem is transformed into convex surrogate using two inertia terms and, then, extended to accommodate noisy measurements. In Section IV, the resulting state estimation and topology identification solution is verified through numerical and experimental benchmarks. Section V concludes the paper.

II. Notations and Terminologies

A. Notations

Throughout this paper, bold uppercase and lowercase letters (e.g., $\boldsymbol{X}$, $\boldsymbol{x}$), refer to the matrices and vectors, respectively.

The authors are supported by the National Science Foundation under award ECCS-1809454. They are with the University of Texas, Arlington, TX, 76019, USA (e-mail: tuncay.altun@mavs.uta.edu; ramtin.madani@uta.edu; davoudi@uta.edu).

$n\times 1$ vectors of zeros and ones are represented by symbols $\mathbf{0}_n$ and $\mathbf{1}_n$, respectively. $\mathbf{0}_{m\times n}$ refers to the $m \times n$ zero matrix. $\boldsymbol{I}_{n\times n}$ is the $n \times n$ identity matrix. The symbol $\mathbb{R}$ defines the sets of real numbers. The matrix entries are presented by indices (i, j). The superscript $(\cdot)^\top$ shows the transpose operator. $|\cdot|$ represents the absolute value of a vector/scalar or the cardinality of a set. $Tr(\cdot)$ refers to the trace of a given matrix. $\|\cdot\|_2$ stands for the euclidean norm of a given vector. $\|\cdot\|_*$ represents the nuclear norm of a given matrix. $\mathrm{diag}\{\cdot\}$ composes a vertical vector from diagonal elements of a given matrix. The notation $\boldsymbol{X} \succeq 0$ means that $\boldsymbol{X}$ is a positive semi-definite matrix.

B. Terminologies

Consider a DC distribution network, where distribution lines are resistive and DC-DC converters interface energy resources to the distribution network as demonstrated in Figure 1. DC network is shown as a directed graph $\mathcal{H} = (\mathcal{N}, \mathcal{L})$, with $\mathcal{N}$ and $\mathcal{L}$ as the sets of buses and lines, respectively. Each bus can accommodate a power electronics converter, a resistive load, and/or a constant power load.

Define the pair $\vec{\boldsymbol{L}}, \overleftarrow{\boldsymbol{L}} \in \{0, 1\}^{|\mathcal{L}|\times|\mathcal{N}|}$ as the *from* and *to* line incidence matrices, respectively. $\vec{\boldsymbol{L}}_{l,i} = 1$ if and only if the line l starts at bus i, and $\overleftarrow{\boldsymbol{L}}_{l,i} = 1$ if and only if the line l ends at bus i. The conductance of a line $l \in \mathcal{L}$ is g_l, with $\boldsymbol{g} \in \mathbb{R}^{|\mathcal{L}|}$ as the line conductance vector. $\boldsymbol{G} \in \mathbb{R}^{|\mathcal{N}|\times|\mathcal{N}|}$ is the bus conductance matrix. $\vec{\boldsymbol{G}}$ and $\overleftarrow{\boldsymbol{G}} \in \mathbb{R}^{|\mathcal{L}|\times|\mathcal{N}|}$ are the *from* and *to* line conductance matrices, respectively.

Let n denote the number of buses, i.e., $n = |\mathcal{N}|$. $\boldsymbol{v} = [v_1, v_2, ..., v_n]^\top$ is the vector of voltages with $v_k \in \mathbb{R}$ as the voltage at bus $k \in \mathcal{N}$. Let $i_k \in \mathbb{R}$ refer to the current-injection at bus $k \in \mathcal{N}$, while $\boldsymbol{i} = [i_1, i_2, ..., i_n]^\top$ is the corresponding vector. Given a line $l \in \mathcal{L}$, there are two current signals, $\vec{\imath}_l \in \mathbb{R}$ and $\overleftarrow{\imath}_l \in \mathbb{R}$, entering the line via its $from$ and to ends, respectively. $\vec{\boldsymbol{\imath}} = [\vec{\imath}_1, \vec{\imath}_2, ..., \vec{\imath}_{|\mathcal{L}|}]^\top$ and $\overleftarrow{\boldsymbol{\imath}} = [\overleftarrow{\imath}_1, \overleftarrow{\imath}_2, ..., \overleftarrow{\imath}_{|\mathcal{L}|}]^\top$ are the vectors of corresponding composites. We assume there is no interlinking converter in the network; hence $\vec{\boldsymbol{\imath}} = -\overleftarrow{\boldsymbol{\imath}}$. $\hat{v}_k$, $\hat{\imath}_k$, and $\hat{x}_l$ denote the measured voltage and the current-injection at bus $k \in \mathcal{N}$, and the status of line $l \in \mathcal{L}$, respectively. v_k and x_l refer to the estimated voltage at bus $k \in \mathcal{N}$, and the identified status of the line $l \in \mathcal{L}$, respectively.

III. Joint State Estimation and Topology Identification

A. Problem Formulation

We will exploit the power flow equations of a DC network to express this problem as a constrained minimization program. The available measurements are: (i) voltage values at some of the randomly-chosen buses, (ii) current-injection values at some of the randomly-chosen buses, and (iii) some of the line statuses. The Ohm's law dictates that the current flow from both sides of each line, and the current-injection at each bus, can be respectively represented as

$$\vec{\boldsymbol{\imath}} = \mathrm{diag}\{\vec{\boldsymbol{G}}\ \boldsymbol{v}\ \boldsymbol{x}^\top\}, \qquad \overleftarrow{\boldsymbol{\imath}} = -\vec{\boldsymbol{\imath}}, \tag{1}$$

$$\boldsymbol{i} = \vec{\boldsymbol{L}}^\top\ \vec{\boldsymbol{\imath}} + \overleftarrow{\boldsymbol{L}}^\top\ \overleftarrow{\boldsymbol{\imath}}. \tag{2}$$

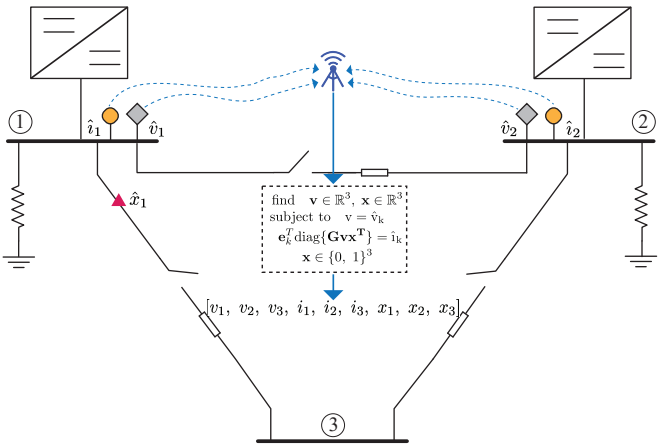

Fig. 1. A portion of a DC distribution network with three buses. The network is endowed with sensors at buses 1 and 2 and the line between buses 1-3 to collect data $(\hat{v}_1, \hat{v}_2, \hat{x}_1, \hat{\imath}_1, \hat{\imath}_2)$. Optimizer jointly performs state estimation and topology identification using these limited measurements, and infers unknown voltage, v_3, and statuses of the lines, x_2, x_3.

Note that (1) and (2) hold true unless there is an interlinking converter on the line.

The state estimation and topology identification algorithm simultaneously finds the voltage vector, $\boldsymbol{v}$, and the line-status vector, $\boldsymbol{x}$, while satisfying all the measurement equations

$$\begin{aligned}
&\text{find} && \boldsymbol{v} \in \mathbb{R}^{|\mathcal{N}|}, \boldsymbol{x} \in \mathbb{R}^{|\mathcal{L}|} && && \text{(3a)}\\
&\text{subject to} && v_k = \hat{v}_k && \forall k \in \mathcal{S}_v && \text{(3b)}\\
& && \boldsymbol{e}_k^\top \mathrm{diag}\{\boldsymbol{G}\boldsymbol{v}\boldsymbol{x}^\top\} = \hat{\imath}_k && \forall k \in \mathcal{S}_i && \text{(3c)}\\
& && \boldsymbol{x}^{\mathrm{lb}} \le \boldsymbol{x} \le \boldsymbol{x}^{\mathrm{ub}} && && \text{(3d)}\\
& && \boldsymbol{x} \in \{0, 1\}^{|\mathcal{L}|} && && \text{(3e)}
\end{aligned}$$

where $\{\boldsymbol{e}_1, ..., \boldsymbol{e}_N\}$ are the basis vectors in $\mathbb{R}^n$. Here, measurement equations refer to the nonlinear relations between sensor outputs and state variables as in (3c). For x^{lb} and x^{ub}, the conditional expressions can be given as

$$\begin{aligned}
&{x_l}^{\mathrm{lb}} = {x_l}^{\mathrm{ub}} = 1, && \text{if line } l \in \mathcal{L} \text{ is known to be connected,}\\
&{x_l}^{\mathrm{lb}} = {x_l}^{\mathrm{ub}} = 0, && \text{if line } l \in \mathcal{L} \text{ is known to be disconnected,}\\
&{x_l}^{\mathrm{lb}} = 0, \quad {x_l}^{\mathrm{ub}} = 1, && \text{if the status of line } l \text{ is undetermined.}
\end{aligned}$$

Here, ${x_l}^{\mathrm{lb}}$ and ${x_l}^{\mathrm{ub}}$ refer to the lower and upper bound of line statuses.

Equation (3b) enforces the voltage value to be equal to the sensor measurement if the corresponding bus is equipped with a voltage sensor (i.e., *a monitored bus*). v_k and $\hat{v}_k$ denote voltage values to be estimated and to be measured for every bus $k \in \mathcal{S}_v$, respectively. $\mathcal{S}_v$ denotes the set of voltage measurements. Equality constraint (3c) aims to find the voltage value and line status that fit the corresponding input value, $\hat{\imath}_k$, from a set of current-injection measurements, $\mathcal{S}_i$. Problem (3) is non-convex because of vector multiplication in $\boldsymbol{v}\boldsymbol{x}^\top$ and the binary variables accounting for the statuses of the lines. In the next section, we offer a convex reformulation for this problem.

B. Convexification of the Problem Formulation

We introduce the following convex optimization problem using the auxiliary variable $\boldsymbol{A}$ accounting for $\boldsymbol{v}\boldsymbol{x}^\top$

$$\underset{\substack{\boldsymbol{A}\in\mathbb{R}^{|\mathcal{N}|\times|\mathcal{L}|}\\ \boldsymbol{v}\in\mathbb{R}^{|\mathcal{N}|}\\ \boldsymbol{x}\in\mathbb{R}^{|\mathcal{L}|}}}{\text{minimize}} \quad \|\boldsymbol{M}^{\frac{1}{2}}(\boldsymbol{A}-\boldsymbol{v}\boldsymbol{x}^\top)\boldsymbol{N}^{\frac{1}{2}}\|_*+\|\boldsymbol{v}-\boldsymbol{v}_0\|^2_{\boldsymbol{M}}+\|\boldsymbol{x}-\boldsymbol{x}_0\|^2_{\boldsymbol{N}} \tag{4a}$$

$$\text{subject to} \quad v_k = \hat{v}_k \qquad \forall k\in\mathcal{S}_v \tag{4b}$$

$$\boldsymbol{e}_k^\top \operatorname{diag}\{\boldsymbol{G}\boldsymbol{A}\} = \hat{\imath}_k \qquad \forall k\in\mathcal{S}_i \tag{4c}$$

$$\boldsymbol{e}_k^\top \boldsymbol{A} = \hat{v}_k\boldsymbol{x}^\top \qquad \forall k\in\mathcal{S}_v \tag{4d}$$

$$\boldsymbol{A}\boldsymbol{d}_l^\top = \boldsymbol{v}\hat{x}_l \qquad \forall l\in\mathcal{S}_x \tag{4e}$$

$$\boldsymbol{x}^{\text{lb}} \le \boldsymbol{x} \le \boldsymbol{x}^{\text{ub}} \tag{4f}$$

$$\boldsymbol{v}\,(\boldsymbol{x}^{\text{lb}})^\top \le \boldsymbol{A} \le \boldsymbol{v}\,(\boldsymbol{x}^{\text{ub}})^\top \tag{4g}$$

where $\boldsymbol{M} \succ 0$ and $\boldsymbol{N} \succ 0$ are arbitrary basis matrices to be designed later. $\{\boldsymbol{d}_1, ..., \boldsymbol{d}_L\}$ are the standard basis vectors in $\mathbb{R}^{|\mathcal{L}|}$. $\boldsymbol{v}_0$ and $\boldsymbol{x}_0$ are the initial guesses for the elements of the voltage and the line-status vectors. They are chosen as 380 V and $\mathbf{1}_n$, respectively, to satisfy flat start operating conditions and imply a fully-connected network.

Notice that the bi-linear term $\boldsymbol{v}\boldsymbol{x}^\top$ in (3c) is replaced by $\boldsymbol{A}$ in (4c) and, therefore, we are dealing with a linear constraint. The nuclear norm term, $\|\boldsymbol{A}-\boldsymbol{v}\boldsymbol{x}^\top\|_*$, implicitly imposes the non-convex equality $\boldsymbol{A} \triangleq \boldsymbol{v}\boldsymbol{x}^\top$ by penalizing the difference.

Proposition 1. *Let $\boldsymbol{v}^*$ and $\boldsymbol{x}^*$ be the solution to (3), and define $\boldsymbol{A}^* \triangleq \boldsymbol{v}^*\boldsymbol{x}^{*\top}$. The constraints in (4d), (4e), and (4g) are valid for $\boldsymbol{A}$, $\boldsymbol{v}$, and $\boldsymbol{x}^\top$.*

Proof. Consider arbitrary voltage and line-status vectors $\boldsymbol{v}$ and $\boldsymbol{x}$, respectively. Let $\boldsymbol{v}^*$ and $\boldsymbol{x}^*$ be the solutions to (3), when voltage and current-injection measurements are chosen from the sets $\mathcal{S}_v$ and $\mathcal{S}_i$, respectively. Constraint (4d) becomes

$$\boldsymbol{e}_k^\top \boldsymbol{A}^* \;=\; \boldsymbol{e}_k\boldsymbol{v}^*\boldsymbol{x}^\top \;=\; v_k\boldsymbol{x}^\top \qquad \forall k\in\mathcal{S}_i. \tag{5}$$

This implies that the constraint (4d) holds for any given $k \in \mathcal{N}$. For every $l \in \mathcal{L}$, (4e) leads to the following equality

$$\boldsymbol{A}^*\boldsymbol{d}_l^\top \;=\; \boldsymbol{v}^*\boldsymbol{x}^\top\boldsymbol{d}_l \;=\; \boldsymbol{v}x_l \qquad \forall l\in\mathcal{S}_x, \tag{6}$$

where it shows that $\boldsymbol{v}x_l$ becomes equivalent to (4e). Similarly, for every $k \in \mathcal{N}$ and $l \in \mathcal{L}$, (4g) becomes

$$x_l{}^{\text{lb}} \le \quad x_l{}^* \quad \le x_l{}^{\text{ub}}, \tag{7a}$$

$$\Rightarrow v_k{}^* x_l{}^{\text{lb}} \le v_k{}^* x_l{}^* \le v_k{}^* x_l{}^{\text{ub}}, \tag{7b}$$

$$\Rightarrow v_k{}^* x_l{}^{\text{lb}} \le \quad A_{kl}{}^* \quad \le v_k{}^* x_l{}^{\text{ub}}. \tag{7c}$$

Note that (4g), (7b), and (7c) are equivalent. Equations (5), (6), and (7) complete the proof for the valid inequalities in (4).

□

Remark 1. *Observe that the nuclear norm term in (4a), $\|\boldsymbol{A}-\boldsymbol{v}\boldsymbol{x}^\top\|_*$ is non-convex. The inertia terms $\|\boldsymbol{v}-\boldsymbol{v}_0\|^2_{\boldsymbol{M}}$ and $\|\boldsymbol{x}-\boldsymbol{x}_0\|^2_{\boldsymbol{N}}$ are added to convexify the overall objective function. This is formally stated by the following theorem.*

Remark 2. *The presence of matrices $\boldsymbol{M}$ and $\boldsymbol{N}$ indicates that the choice of basis can be arbitrary. We will demonstrate how $\boldsymbol{M}$ and $\boldsymbol{N}$ can boost the convergence rate of the proposed approach. A penalty term induced by a physical quantity, such as loss, can help address the non-convexity.*

Theorem 1. *The function $f : \mathbb{R}^{n\times l} \times \mathbb{R}^n \times \mathbb{R}^l \to \mathbb{R}$, defined as*

$$f(\boldsymbol{A},\boldsymbol{v},\boldsymbol{x}) \triangleq \|\boldsymbol{M}^{\frac{1}{2}}(\boldsymbol{A}-\boldsymbol{v}\boldsymbol{x}^\top)\boldsymbol{N}^{\frac{1}{2}}\|_*+\|\boldsymbol{v}-\boldsymbol{v}_0\|^2_{\boldsymbol{M}}+\|\boldsymbol{x}-\boldsymbol{x}_0\|^2_{\boldsymbol{N}}, \tag{8}$$

is convex.

Proof. Define new variables $\boldsymbol{B} \triangleq \boldsymbol{M}^{\frac{1}{2}}\boldsymbol{A}\boldsymbol{N}^{\frac{1}{2}}$, $\boldsymbol{s} \triangleq \boldsymbol{M}^{\frac{1}{2}}\boldsymbol{v}$, and $\boldsymbol{r} \triangleq \boldsymbol{N}^{\frac{1}{2}}\boldsymbol{x}$. It suffices to show that the following function is convex:

$$g(\boldsymbol{B},\boldsymbol{s},\boldsymbol{r}) \triangleq \|\boldsymbol{B}-\boldsymbol{s}\boldsymbol{r}^\top\|_* + \|\boldsymbol{s}\|_2^2 + \|\boldsymbol{r}\|_2^2. \tag{9}$$

According to triangle inequality we have:

$$g(\boldsymbol{\Lambda},\boldsymbol{\nu},\boldsymbol{\xi}) - \theta g(\boldsymbol{B}_1,\boldsymbol{s}_1,\boldsymbol{r}_1) - (1-\theta)g(\boldsymbol{B}_2,\boldsymbol{s}_2,\boldsymbol{r}_2) \le 0, \tag{10}$$

where $\boldsymbol{\Lambda}$, $\boldsymbol{\nu}$, and $\boldsymbol{\xi}$ are

$$\boldsymbol{\Lambda} = \theta\boldsymbol{B}_1 + (1-\theta)\boldsymbol{B}_2, \tag{11a}$$

$$\boldsymbol{\nu} \;=\; \theta\boldsymbol{s}_1 + (1-\theta)\boldsymbol{s}_2, \tag{11b}$$

$$\boldsymbol{\xi} \;=\; \theta\boldsymbol{r}_1 + (1-\theta)\boldsymbol{r}_2. \tag{11c}$$

The inequality in (10) can be expanded as

$$\begin{aligned}\|\boldsymbol{\Lambda}-[\boldsymbol{\nu}][\boldsymbol{\xi}]^\top\|_* - \theta\|\boldsymbol{B}_1-\boldsymbol{s}_1\boldsymbol{r}_1^\top\|_* - (1-\theta)\|\boldsymbol{B}_2-\boldsymbol{s}_2\boldsymbol{r}_2^\top\|_* \\ \le \|\theta\boldsymbol{s}_1\boldsymbol{r}_1^\top + (1-\theta)\boldsymbol{s}_2\boldsymbol{r}_2^\top - [\boldsymbol{\nu}][\boldsymbol{\xi}]^\top\|_* \\ = \theta(1-\theta)\|\boldsymbol{s}_1-\boldsymbol{s}_2\|_2\|\boldsymbol{r}_1-\boldsymbol{r}_2\|_2.\end{aligned} \tag{12}$$

Further simplification of (12) leads to

$$\begin{aligned}\|\boldsymbol{\nu}\|_2^2+\|\boldsymbol{\xi}\|_2^2 - \theta(\|\boldsymbol{s}_1\|_2^2+\|\boldsymbol{r}_1\|_2^2) - (1-\theta)(\|\boldsymbol{s}_2\|_2^2+\|\boldsymbol{r}_2\|_2^2) \\ = -\theta(1-\theta)[\|\boldsymbol{s}_1-\boldsymbol{s}_2\|_2^2 + \|\boldsymbol{r}_1-\boldsymbol{r}_2\|_2^2],\end{aligned} \tag{13}$$

which completes the proof of *Theorem 1*. □

C. The Choice of Basis Matrices

The original problem in (3) has been expressed as a convex optimization problem (4) with basis matrices $\boldsymbol{M}$ and $\boldsymbol{N}$. These basis matrices should be chosen properly such that the solution to (4) satisfies the problem in (3). Inspired by [12], matrix $\boldsymbol{M}$ is chosen to represent the network's total power loss.

Power flow on a line $l \in \mathcal{L}$ can be calculated for the two neighboring buses $(i, j) \in \mathcal{N}$ as

$$\vec{p}_l = v_i(v_i - v_j)g_l x_l, \tag{14a}$$

$$\overleftarrow{p}_l = v_j(v_j - v_i)g_l x_l, \tag{14b}$$

where $\vec{p}_l$ and $\overleftarrow{p}_l$ denote the power flow from the starting and ending sides of each line $l \in \mathcal{L}$. Power loss on a line is

$$\vec{p}_l + \overleftarrow{p}_l = v_i(v_i - v_j)g_l x_l + v_j(v_j - v_i)g_l x_l \tag{15a}$$

$$= \quad (v_i{}^2 - v_i v_j + v_j{}^2 - v_i v_j)g_l x_l \tag{15b}$$

$$= \quad (v_i{}^2 + v_j{}^2 - 2v_iv_j)g_lx_l \tag{15c}$$
$$= \quad (v_i - v_j)(g_lx_l)(v_i - v_j)^\top. \tag{15d}$$

The total power loss is the sum of power flows entering the lines through their starting and ending buses as

$$\vec{\boldsymbol{p}} = \mathrm{diag}\{\vec{\boldsymbol{L}}\ \boldsymbol{v}\ \boldsymbol{v}^\top\ \vec{\boldsymbol{G}}^\top\}, \quad \overleftarrow{\boldsymbol{p}} = \mathrm{diag}\{\overleftarrow{\boldsymbol{L}}\ \boldsymbol{v}\ \boldsymbol{v}^\top\ \overleftarrow{\boldsymbol{G}}^\top\} \tag{16a}$$
$$\sum(\vec{\boldsymbol{p}} + \overleftarrow{\boldsymbol{p}}) = Tr(\boldsymbol{v}\ \boldsymbol{v}^\top(\vec{\boldsymbol{G}}^\top\ \vec{\boldsymbol{L}} + \overleftarrow{\boldsymbol{G}}^\top\ \overleftarrow{\boldsymbol{L}})) \tag{16b}$$
$$= \boldsymbol{v}^\top\ (\vec{\boldsymbol{G}}^\top\ \vec{\boldsymbol{L}} + \overleftarrow{\boldsymbol{G}}^\top\ \overleftarrow{\boldsymbol{L}})\ \boldsymbol{v}. \tag{16c}$$

Using (16c), we can chose $\boldsymbol{M}$ as

$$\boldsymbol{M} = (\vec{\boldsymbol{G}}^\top\ \vec{\boldsymbol{L}} + \overleftarrow{\boldsymbol{G}}^\top\ \overleftarrow{\boldsymbol{L}}). \tag{17}$$

Notice that if $\boldsymbol{M}$ is chosen as in (17), which is actually equal to the conductance matrix $\boldsymbol{G}$, loss minimization will be indirectly embedded in the objective function (4a) with a proper choice of $\boldsymbol{N}$. $\boldsymbol{N} = \boldsymbol{I}_{l\times l}$ implicitly penalizes the power loss over all the lines as given in (15).

D. Strengthening the Convex Relaxation

Power networks usually have intermediate buses (or hidden nodes [13]) that do not demand/supply power or current with any external source or load, e.g., see bus 3 in Figure 1. These intermediate buses are referred to as *zero injection buses* [26]. We exploit their presence to define a number of valid inequality and strengthen the convex relaxation in (4).

Definition 1. *A bus $k \in \mathcal{N}$ is regarded as a zero injection bus if both power and current injections at bus k are zero, i.e.,if no load or source is located at the bus [12]. The set of zero injection buses are presented by $\mathcal{Z}$.*

Proof. Let $\boldsymbol{v}^*$ and $\boldsymbol{x}^*$ be the solutions to the original problem (3). Then,

$$\boldsymbol{e}_k^\top \mathrm{diag}\{\boldsymbol{G}\boldsymbol{v}^*\boldsymbol{x}^{*\top}\} = \boldsymbol{0}_n \tag{18}$$

holds for every $k \in \mathcal{Z}$, where $n = |\mathcal{Z}|$.

For zero injection buses, the sum of the currents absorbed from the distribution network is equal to the sum of the currents they supply to the distribution network. This feature can be expressed as

$$\boldsymbol{e}_k^\top \mathrm{diag}\{\boldsymbol{G}\boldsymbol{v}^*\boldsymbol{x}^{*\top}\} = \sum_{l=1}^{|\mathcal{K}|} d_l^\top(\vec{\boldsymbol{L}}\ \mathrm{diag}\{\vec{\boldsymbol{G}}\boldsymbol{v}^*\boldsymbol{x}^{*\top}\} + \overleftarrow{\boldsymbol{L}}\ \mathrm{diag}\{\overleftarrow{\boldsymbol{G}}\boldsymbol{v}^*\boldsymbol{x}^{*\top}\}), \tag{19}$$

where $\mathcal{K}$ denotes the set of neighboring buses of the zero injection bus k. The following formulation can be inferred from (19)

$$\sum_{l=1}^{|\mathcal{K}|} d_l^\top(\vec{\boldsymbol{L}}\ \mathrm{diag}\{\vec{\boldsymbol{G}}\boldsymbol{v}^*\boldsymbol{x}^{*\top}\}) = -\sum_{l=1}^{|\mathcal{K}|} d_l^\top(\overleftarrow{\boldsymbol{L}}\ \mathrm{diag}\{\overleftarrow{\boldsymbol{G}}\boldsymbol{v}^*\boldsymbol{x}^{*\top}\}), \tag{20}$$

concluding that (18) is valid for any $k \in \mathcal{Z}$. □

According to (20), the set of additional constraints

$$\boldsymbol{e}_k^\top \mathrm{diag}\{\boldsymbol{G}\boldsymbol{A}\} = \boldsymbol{0}_n \tag{21}$$

can be added in (4) to strengthen its relaxation.

E. Estimation in the Presence of Noisy Measurements

The convex problem (4) can become infeasible, or result in a poor approximate, if available measurements become noisy. In this case, solving the state estimation problem requires tackling two concerns: (i) how to address non-linear relation between sensor measurements and state variables, (ii) how to address corrupted sensor measurements. We introduce auxiliary variables $\boldsymbol{o} \in \mathbb{R}^{|\mathcal{N}|}$ and $\boldsymbol{a} \in \mathbb{R}^{|\mathcal{L}|}$ to handle measurement noise. A new variable $\boldsymbol{u} \in \mathbb{R}^{|\mathcal{N}|}$ accounts for the $\boldsymbol{o}^2$. Unknown measurement noise can be estimated by incorporating these auxiliary variables as convex regularization terms into the objective function (4a). The DC network state estimation problem for a static distribution network, that is robust to noisy measurements, can be formulated as

$$\underset{\substack{\boldsymbol{A}\in\mathbb{R}^{|\mathcal{N}|\times|\mathcal{L}|}\\ \boldsymbol{u},\boldsymbol{v},\boldsymbol{o}\in\mathbb{R}^{|\mathcal{N}|}\\ \boldsymbol{x},\boldsymbol{a}\in\mathbb{R}^{|\mathcal{L}|}}}{\text{minimize}} \quad \|\boldsymbol{M}^{\frac{1}{2}}(\boldsymbol{A}-\boldsymbol{v}\boldsymbol{x}^\top)\boldsymbol{N}^{\frac{1}{2}}\|_* + \|\boldsymbol{v}-\boldsymbol{v}_0\|_{\boldsymbol{M}}^2 + \|\boldsymbol{x}-\boldsymbol{x}_0\|_{\boldsymbol{N}}^2 + \mu_1(\boldsymbol{1}^\top\boldsymbol{u}) + \mu_2\|\boldsymbol{a}\|_2^2 \tag{22a}$$

$$\text{subject to} \quad v_k = \hat{v}_k - o_k \qquad \forall k\in\mathcal{S}_v \tag{22b}$$

$$\boldsymbol{e}_k^\top \mathrm{diag}\{\boldsymbol{G}\boldsymbol{A}\} = \hat{\imath}_k - a_k \qquad \forall k\in\mathcal{S}_i \tag{22c}$$
$$\boldsymbol{A}\ \boldsymbol{d}_l^\top = \boldsymbol{v}\ \hat{x}_l \qquad \forall l\in\mathcal{S}_x \tag{22d}$$
$$\boldsymbol{x}^{\mathrm{lb}} \le \boldsymbol{x} \le \boldsymbol{x}^{\mathrm{ub}} \tag{22e}$$
$$\boldsymbol{v}\,(\boldsymbol{x}^{\mathrm{lb}})^\top \le \boldsymbol{A} \le \boldsymbol{v}\,(\boldsymbol{x}^{\mathrm{ub}})^\top \tag{22f}$$
$$o_k^2 \le u_k \qquad \forall k\in\mathcal{S}_v \tag{22g}$$

$$\begin{bmatrix} x_l & \hat{v}_kx_l - A_{kl} \\ \hat{v}_kx_l - A_{kl} & u_k \end{bmatrix} \succeq 0 \quad \forall k\in\mathcal{S}_v,\ \ \forall l\in\mathcal{L} \tag{22h}$$

where $\mu_1 \ge 0$ and $\mu_2 \ge 0$ are pre-selected coefficients that balance the data fitting cost $\mu_1(\boldsymbol{1}^\top\boldsymbol{u}) + \mu_2\|\boldsymbol{a}\|_2^2$ with the remaining elements of the objective function in (22a). The objective function (4a) aims to handle the non-linearity of the measurement equation, while convex regularization term added in (22a) deals with the noisy measurements.

Proposition 2. *Let $\boldsymbol{v}^*$, $\boldsymbol{x}^*$, $\boldsymbol{o}^*$, and $\boldsymbol{u}^*$ be the ground-truth values for the original problem (3). Let $\boldsymbol{u}^* \triangleq \boldsymbol{o}^{*2}$ and $\boldsymbol{A}^* \triangleq \boldsymbol{v}^*\boldsymbol{x}^{*\top}$. Then, the constraint (22h) is satisfied.*

Proof. Since v_k^* and x_l^* are positive, one can write

$$A_{kl}^* = v_k^*x_l^* \Leftrightarrow A_{kl}^* = (\hat{v}_k - o_k^*)x_l^* \tag{23a}$$
$$\Rightarrow\ \hat{v}_kx_l^* - A_{kl}^* = o_k^*x_l^* \Leftrightarrow (\hat{v}_kx_l^* - A_{kl}^*)^2 = o_k^{*2}x_l^{*2} \tag{23b}$$
$$\Rightarrow (\hat{v}_kx_l^* - A_{kl}^*)^2 = u_k^*x_l^* \Leftrightarrow (\hat{v}_kx_l^* - A_{kl}^*)^2 \le u_k^*x_l^* \tag{23c}$$

As seen, (23) is equivalent to (22h) under the proposition 3. This completes the proof. □

If pre-selected coefficients are chosen as $\mu_1 = 0$ and $\mu_2 = 0$, the objective function (22a) is reduced to the objective function (4a), which can only contrive the non-convexity of the measurement equations in noiseless scenarios. If $\mu_1 = +\infty$ and $\mu_2 = +\infty$, then the objective function (22a) prioritizes estimating the unknown noise values while ignoring the remaining elements.

It should be noted that the goal is to find an approximate solution for the state estimation problem in the presence of noisy measurements without increasing the number of available sensors. Alternatively, (22) could cleanse all the noise on measurements with the help of redundant sensor.

IV. Case Studies

In the following, standard IEEE AC benchmarks are transformed into DC benchmarks by replacing AC generators with DC-DC converters, and making distribution lines purely resistive. All lines are equipped with switches to control the network topology. If monitored, a bus is equipped with a sensor to measure voltage and/or a sensor to measure current injection. Monitored lines refer to the lines with a sensor. The optimization problem is run using the conic interior-point solver, MOSEK [27], in the CVX [28] optimization package.

A. Numerical Studies

The joint state estimation and topology identification problem is examined for the modified IEEE 9-bus, 14-bus, and 30-bus systems [29]. We compare our method in (4), using proper basis $\boldsymbol{M}$ and $\boldsymbol{N}$ values in (17) and the set of additional constraints in (21), with the conventional GSE method [4]. Each simulation has a time horizon with 100 steps; random changes in voltage levels and an arbitrary line removal happen at every time-step and every fifth time-step, respectively. This 100-run simulation is repeated as the total number of sensors increases. Each approach has a flat start with 10^{-6} as the mismatch threshold to conclude a successful run. The success of the GSE method hinges on a full observability condition that would require highly-redundant sensor allocation. As seen in Figures 2 (a)-(c), the proposed method significantly outperforms the GSE approach.

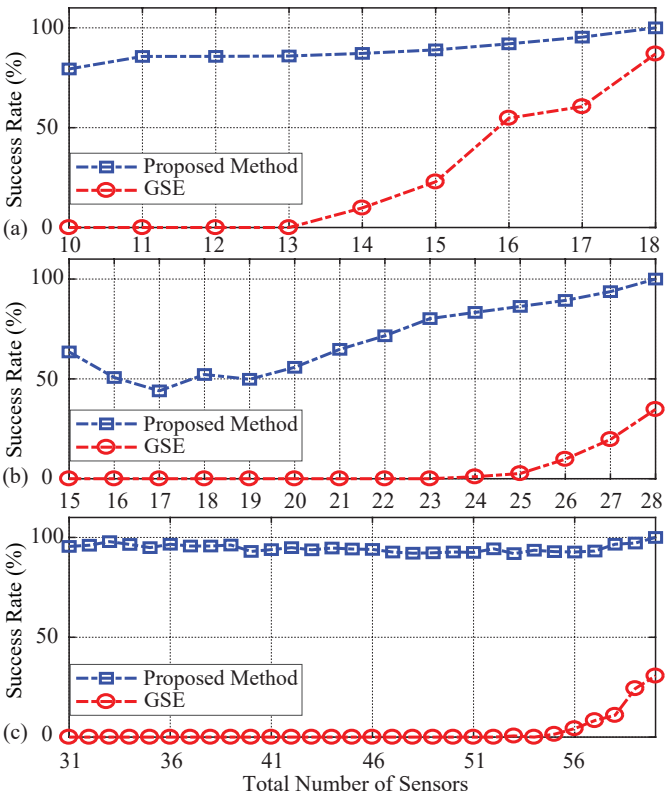

Fig. 2. Comparative convergence rates of proposed and generalized state estimation methods for the IEEE (a) 9-bus, (b) 14-bus, and (c) 30 bus systems.

B. Experimental Studies

In the modified 14-bus system, the input voltage of DC-DC buck converters is 500 V, while the distribution network is rated for 380 V. The ratings of the power converters located at buses 1, 2, 3, 6, and 8 are 150 kW, 50 kW, 100 kW, 100 kW, and 50 kW, respectively. Sample consumption trajectories for the six out of eleven loads are given in Figure 4. The consumption profiles intentionally mimic a 24-hour load pattern, and are generated using poisson distribution. This distribution assumes that the sudden load changes occur randomly with the probability mass function, $P(k) = e^{-\lambda}\frac{\lambda^k}{k!}$. Here, k and λ denote the type and average number of load changes. The voltage sensors are placed on the buses with a power converter. The current injection values are measured for buses ($\mathcal{N} \setminus \mathcal{Z}$) that are not zero-injection buses. It should be observed that bus 7 and bus 14 of the IEEE-14 bus system are zero injection buses. The statuses of ten lines are monitored as illustrated in Figure 3. The internal droop mechanism of power converters regulate their output voltage in response to output power variations due to the changes in the load profile or network topology. This network is emulated in a HIL environment, with a dSPACE DS 1202 MicroLabBox to implement droop controllers for individual converters, and a Typhoon HIL 604 unit to emulate power converters and the distribution network. The proposed optimization algorithm runs on a 16-core Xeon PC with 256 GB RAM.

1) Noiseless measurements: We consider a time horizon, where the statuses of unmonitored lines change randomly and load profiles are dynamic. The proposed formulation in (4), with $\boldsymbol{M} = \boldsymbol{G}$, $\boldsymbol{N} = \boldsymbol{I}_{l\times l}$, and the set of additional constraints in (21), finds states and topology configurations every five seconds. Figure 6 shows the recovered (v) and the ground-truth ($\tilde{v}$) voltage values for the unmonitored buses. Figure 7 presents the recovered (x) and the ground truth ($\tilde{x}$) values for the statuses of unmonitored lines in response to the removal of an arbitrary line. It can be seen that the proposed method yields a very good pursuit of ground-truth values for voltages and statuses of the lines when measurements are assumed noiseless. So far, we haven't used any penalty term or tuning parameter in the convex program (4). The average time for finding states and topology configurations is 2.208 sec.

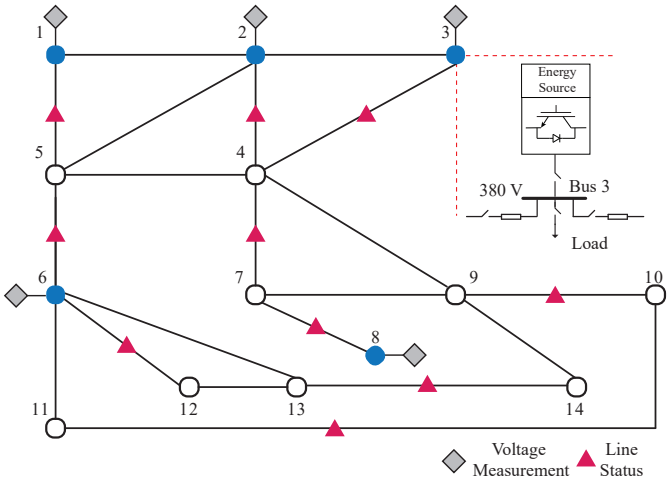

Fig. 3. The IEEE 14-bus system augmented with 5 converters at buses 1, 2, 3, 6, and 8 (shown by ●), and equipped with sensors to monitor voltages (shown by ◆), line statuses (shown by ▲), and injected current at bus $k \in \mathcal{N} \setminus \{\mathcal{Z}\}$.

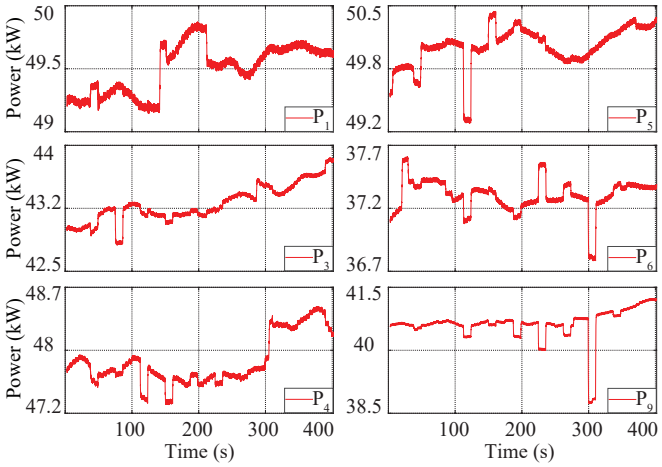

Fig. 4. Load power trajectories at selected buses 1, 3, 4, 5, 6, and 9.

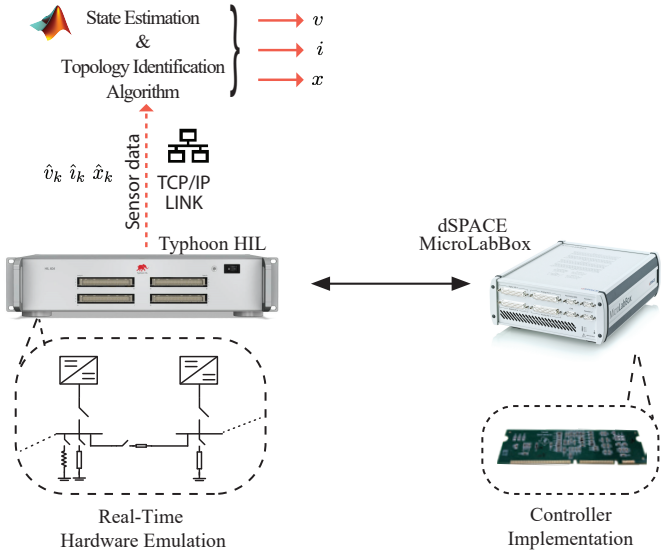

Fig. 5. DC network joint observation testbed on a HIL system consisting of the real-time hardware emulation (Typhoon HIL), controller implementation (dSPACE), and TCP/IP communication link for data transfer.

2) Noisy measurements: All the voltage and current measurements are corrupted by zero-mean Gaussian noises with 1% standard deviation of the corresponding noiseless value. The proposed formulation in (22), with $\boldsymbol{M} = \boldsymbol{G}$ and $\boldsymbol{N} = \boldsymbol{I}_{l\times l}$, finds system states every five seconds. The pre-selected coefficients in (22), that balance the data fitting cost, are set to $\mu_1 = 10^4$ and $\mu_2 = 10^{-2}$. These coefficients improve the accuracy of the noise estimation on voltages ($\boldsymbol{u}$) and currents ($\boldsymbol{a}$). Here, root-mean-square error (RMSE) is considered as a performance metric to assess the estimated voltages $\boldsymbol{v}$ under the zero-mean Gaussian noise that has 1% standard deviation for all the measurements. The RMSE of the $\boldsymbol{v}$ is formalized as $\psi(\boldsymbol{v}) := \|\boldsymbol{v}-\tilde{\boldsymbol{v}}\|_2/\|\tilde{\boldsymbol{v}}\|_2^2$. The RMSE of the estimated voltages obtained by (22), shown in Figure 8, demonstrates that approximate solution is recoverable with 99.85% accuracy. Figure 9 shows the corrupted ($\hat{v}$), recovered (v), and the ground truth ($\tilde{v}$) voltage values where bus measurements are corrupted by 1%. It can be seen that the proposed method yields a very close pursuit of ground-truth voltage values when all the voltage and current measurements are subject to noise. Determination of states in the presence of noisy measurements takes 2.653 sec on average.

V. Conclusion

This paper offers a convex optimization framework to solve the joint state estimation and topology identification problem using only a limited number of measurement for converter-augmented DC networks. This problem is formulated as a constrained minimization problem, where a proper choice of objective function obviates any tuning coefficient in the absence of measurement noise. The problem formulation is then extended for the noisy measurements by adding auxiliary variables to account for convex regularization terms in the objective function. The proposed method is studied where the set of measurements are: (i) voltage values at some of the randomly-chosen buses, (ii) current-injection values at some of the randomly-chosen buses, and (iii) some of the line statuses. The convex formulation in the absence of measurement noise is validated through numerical tests using IEEE 9-bus, 14-bus, and 30-bus benchmarks, and HIL experimentation using modified IEEE 14-bus system. Furthermore, the solution in the presence of 1% measurement noise is verified through HIL experimentation on the IEEE 14-bus system.

VI. Acknowledgment

We are thankful to dSPACE Inc. and Typhoon HIL Inc. for allowing us to use the images of their products.

References

[1] A. Monticelli, "Electric power system state estimation," *Proceedings of the IEEE*, vol. 88, no. 2, pp. 262–282, Feb 2000.
[2] E. Caro, A. J. Conejo, and A. Abur, "Breaker status identification," *IEEE Transactions on Power Systems*, vol. 25, no. 2, pp. 694–702, May 2010.
[3] G. N. Korres and P. J. Katsikas, "Identification of circuit breaker statuses in wls state estimator," *IEEE Transactions on Power Systems*, vol. 17, no. 3, pp. 818–825, Aug 2002.
[4] O. Alsac, N. Vempati, B. Stott, and A. Monticelli, "Generalized state estimation," *IEEE Transactions on Power Systems*, vol. 13, no. 3, pp. 1069–1075, Aug 1998.

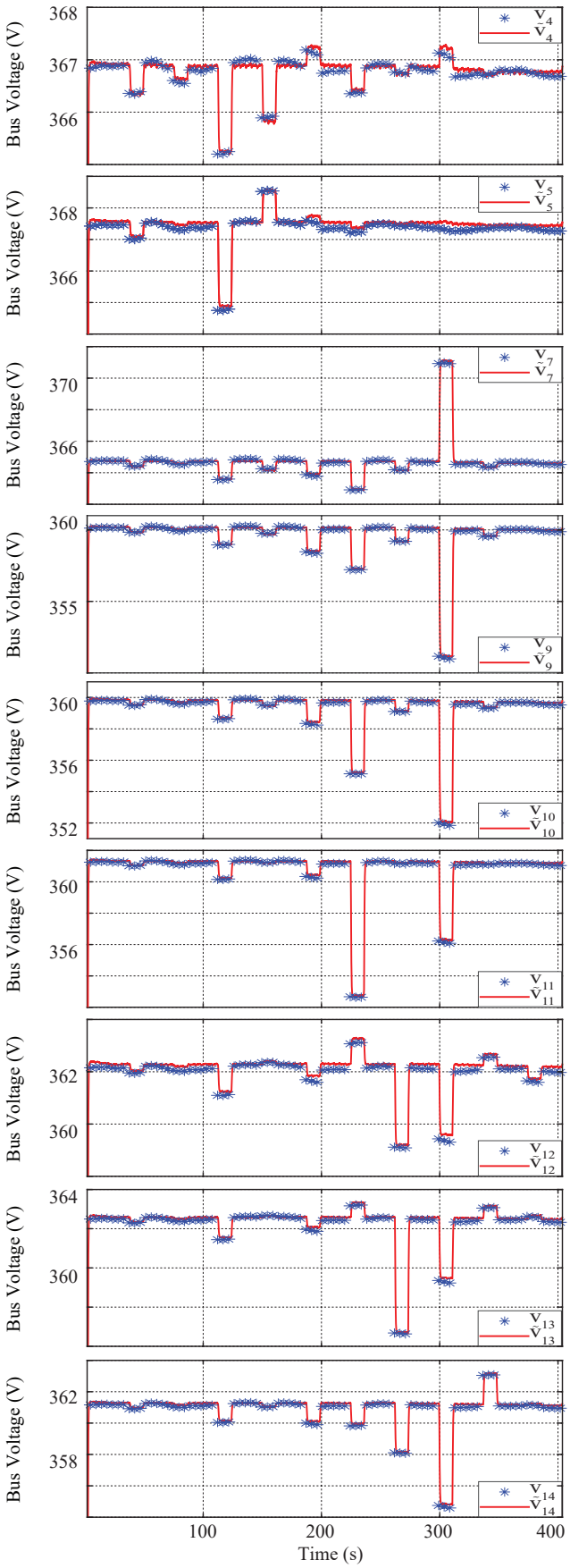

Fig. 6. Estimated (v_k), and ground truth ($\tilde{v}_k$) voltage values for unmonitored buses.

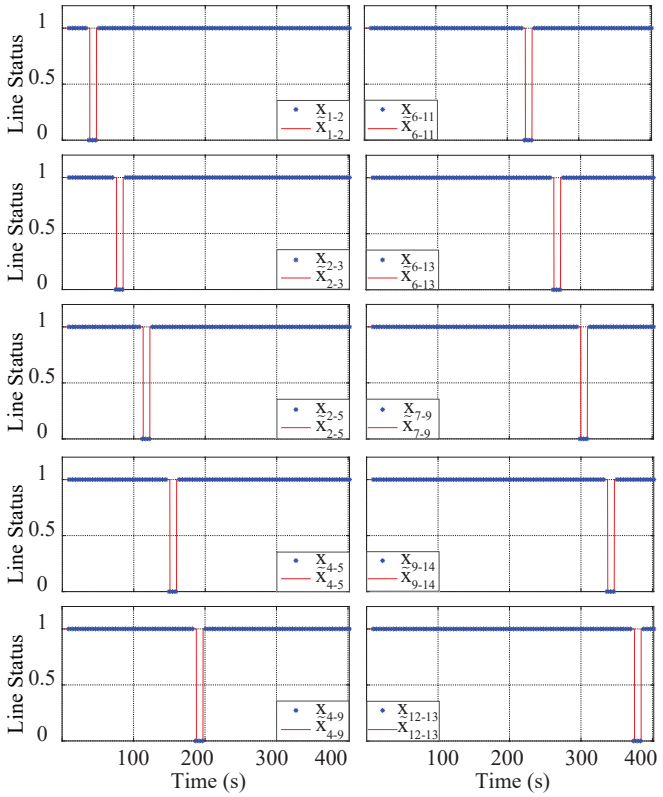

Fig. 7. Estimated (x_l), and ground truth ($\tilde{x}_l$) values for the statuses of the lines in response to the removal of one line. x_{a-b} denotes the line status for a line which starts from node a and ends in b.

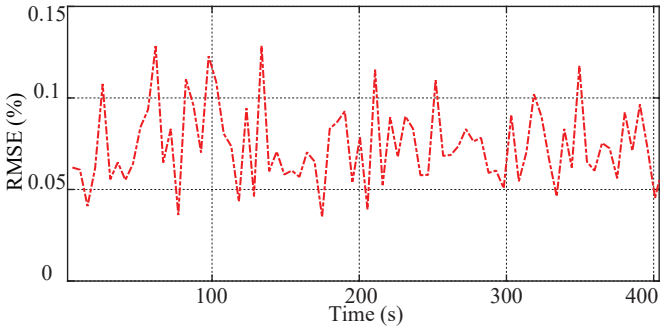

Fig. 8. The performance of (22) to estimate vector of voltages for the modified IEEE-14 bus system under %1 measurement noise.

[5] V. Kekatos and G. B. Giannakis, "Joint power system state estimation and breaker status identification," in *2012 North American Power Symposium (NAPS)*, Sep. 2012, pp. 1–6.

[6] A. Gomez-Exposito and A. Abur, *Power System State Estimation: Theory and Implementation*. CRC press, 2004.

[7] H. Zhu and G. B. Giannakis, "Estimating the state of ac power systems using semidefinite programming," in *2011 North American Power Symposium*, Aug 2011, pp. 1–7.

[8] Y. Weng, Q. Li, R. Negi, and M. Ilić, "Semidefinite programming for power system state estimation," in *2012 IEEE Power and Energy Society General Meeting*, July 2012, pp. 1–8.

[9] Y. Zhang, R. Madani, and J. Lavaei, "Conic relaxations for power system state estimation with line measurements," *IEEE Transactions on Control of Network Systems*, vol. 5, no. 3, pp. 1193–1205, Sep. 2018.

[10] R. Madani, J. Lavaei, R. Baldick, and A. Atamtürk, "Power system state estimation and bad data detection by means of conic relaxation," in *Proceedings of the 50th Hawaii International Conference on System Sciences*, 2017.

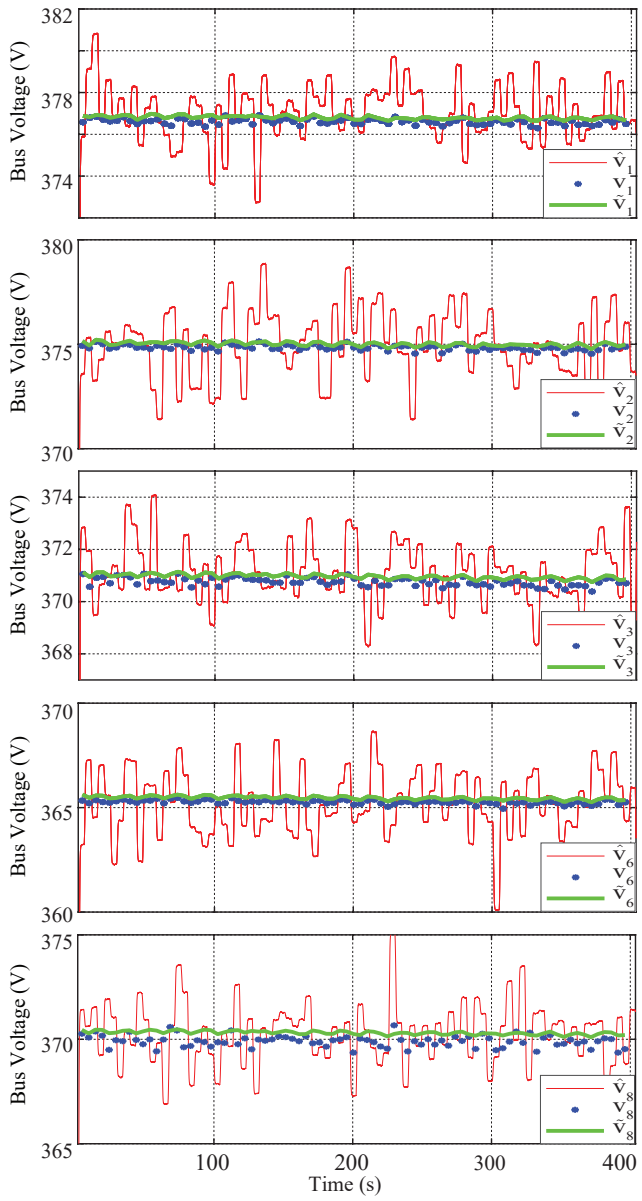

Fig. 9. Estimated voltage values obtained by (22) for the monitored sensor measurements are corrupted by %1 additive noise.

[11] R. Madani, M. Ashraphijuo, J. Lavaei, and R. Baldick, "Power system state estimation with a limited number of measurements," in *2016 IEEE 55th Conference on Decision and Control (CDC)*, Dec 2016, pp. 672–679.

[12] R. Madani, J. Lavaei, and R. Baldick, "Convexification of power flow equations in the presence of noisy measurements," *IEEE Transactions on Automatic Control*, pp. 1–1, 2019.

[13] Y. Yuan, O. Ardakanian, S. Low, and C. Tomlin, "On the inverse power flow problem," *arXiv preprint arXiv:1610.06631*, 2016.

[14] S. Bhela, V. Kekatos, and S. Veeramachaneni, "Enhancing observability in distribution grids using smart meter data," *IEEE Transactions on Smart Grid*, vol. 9, no. 6, pp. 5953–5961, Nov 2018.

[15] K. A. Clements, "The impact of pseudo-measurements on state estimator accuracy," in *2011 IEEE Power and Energy Society General Meeting*, July 2011, pp. 1–4.

[16] K. Dehghanpour, Z. Wang, J. Wang, Y. Yuan, and F. Bu, "A survey on state estimation techniques and challenges in smart distribution systems," *IEEE Transactions on Smart Grid*, vol. 10, no. 2, pp. 2312–2322, March 2019.

[17] A. J. Schmitt, A. Bernstein, and Y. Zhang, "Matrix completion for low-observability voltage estimation," *arXiv preprint arXiv:1801.09799*, 2018.

[18] J. Comden, A. Bernstein, and Z. Liu, "Sample complexity of power system state estimation using matrix completion," *arXiv preprint arXiv:1905.01789*, 2019.

[19] Y. Sharon, A. M. Annaswamy, A. L. Motto, and A. Chakraborty, "Topology identification in distribution network with limited measurements," in *2012 IEEE PES Innovative Smart Grid Technologies (ISGT)*, Jan 2012, pp. 1–6.

[20] L. Zhao, W. Song, L. Tong, Y. Wu, and J. Yang, "Topology identification in smart grid with limited measurements via convex optimization," in *2014 IEEE Innovative Smart Grid Technologies - Asia (ISGT ASIA)*, May 2014, pp. 803–808.

[21] A. Primadianto and C. Lu, "A review on distribution system state estimation," *IEEE Transactions on Power Systems*, vol. 32, no. 5, pp. 3875–3883, Sep. 2017.

[22] J. Zhao, A. Gomez-Exposito, M. Netto, L. Mili, A. Abur, V. Terzija, I. Kamwa, B. C. Pal, A. K. Singh, J. Qi, Z. Huang, and A. P. S. Meliopoulos, "Power system dynamic state estimation: Motivations, definitions, methodologies and future work," *IEEE Transactions on Power Systems*, pp. 1–1, 2019.

[23] G. Fiore, A. Iovine, E. De Santis, and M. D. Di Benedetto, "Secure state estimation for dc microgrids control," in *2017 13th IEEE Conference on Automation Science and Engineering (CASE)*, Aug 2017, pp. 1610–1615.

[24] W. Doorsamy and W. A. Cronje, "State estimation on stand-alone dc microgrids through distributed intelligence," in *2015 International Conference on Renewable Energy Research and Applications (ICRERA)*, Nov 2015, pp. 227–231.

[25] M. Angjelichinoski, . Stefanović, P. Popovski, A. Scaglione, and F. Blaabjerg, "Topology identification for multiple-bus dc microgrids via primary control perturbations," in *2017 IEEE Second International Conference on DC Microgrids (ICDCM)*, June 2017, pp. 202–206.

[26] K. Gharani Khajeh, E. Bashar, A. Mahboub Rad, and G. B. Gharehpetian, "Integrated model considering effects of zero injection buses and conventional measurements on optimal pmu placement," *IEEE Transactions on Smart Grid*, vol. 8, no. 2, pp. 1006–1013, March 2017.

[27] M. ApS, *The MOSEK optimization toolbox for MATLAB manual. Version 8.1.*, 2017. [Online]. Available: http://docs.mosek.com/8.1/toolbox/index.html

[28] M. Grant and S. Boyd, "CVX: Matlab software for disciplined convex programming, version 2.1," http://cvxr.com/cvx, Mar. 2014.

[29] R. D. Zimmerman, C. E. Murillo-Sanchez, and R. J. Thomas, "Matpower: Steady-state operations, planning, and analysis tools for power systems research and education," *IEEE Transactions on Power Systems*, vol. 26, no. 1, pp. 12–19, Feb 2011.